Pergamon

Tetrahedron Vol. 51, No. 4, pp. 1301-1310, 1995

0040-4020/95 $9.50+0.00

0040-4020(94)01022-6

The Conformation of Aldisin and Analogues. A Potential Model for Expanded Nucleosides.

Shamil Latypov†, Rogelio Fernández, Emilio Quiñoá and Ricardo Riguera*

Departamento de Química Orgánica. Facultad de Química. Santiago de Compostela. España.

Abstract: DNMR experiments and MM and AM1 calculations were carried out on aldisin derivatives **6-9** and on the heterocyclic part of expanded nucleosides **1-5.** Aldisines **6-9** present in solution a distorted twist-boat conformation like that of azepinomycin (**3**) while coformycin (**1**), pentostatin (**2**), **4** and **5** have a slight preference for a boat conformation. The proximity in geometry and interconversion barrier suggest that **6-9** can be considered as models for new expanded nucleosides.

Naturally occurring antibiotics coformycin (**1**) and pentostatin (2'-deoxycoformycin), (**2**)[1] are nucleoside analogues containing an imidazo [4,5-e][1,3] diazepine system. Both **1** and **2** structurally resemble the transition state of adenosine during its deamination to inosine by adenosine deaminase (ADA),[2] and are thus powerful inhibitors of the latter enzyme. X-ray diffraction studies of the enzyme-substrate complex have been obtained[3] and the role of the helical structure of the polynucleotide evaluated[4].

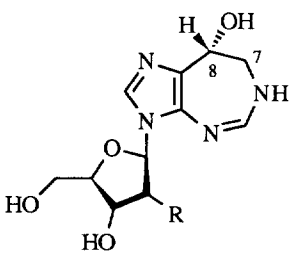

1 R=OH Coformycin
2 R=H Pentostatin

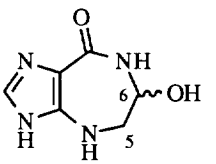

3 Azepinomycin

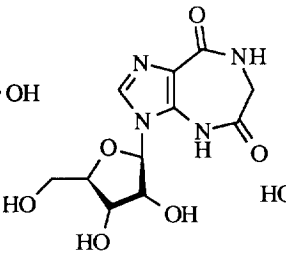

4

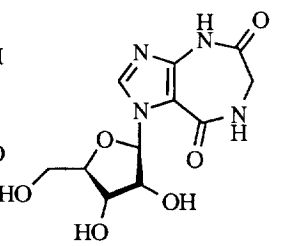

5

The discovery that **1** and **2** can also act as synergistic antitumour agents has stimulated interest in the synthesis and structural and biological evaluation of other "ring-expanded" nucleosides and the corresponding nucleotides and polynucleotides[5]. In the search for new and more potent inhibitors of ADA, several structurally modified versions of **1** and **2** have been prepared, among them compounds containing a pyrazole or [1,2,3] triazole ring[6] instead of imidazole, or a [1, 4] diazepine[7] or [1, 2, 4] triazepine[8] ring instead of the [1, 3] diazepine, e.g. imidazodiazepinone (**3**) (azepinomycin)[9] and imidazodiazepinediones (**4**) and (**5**); the latter compound is a potent inhibitor of murine leukemia virus reverse transcriptase[5].

† On leave from The Institute of Organic&Physical Chemistry of Russian Academy of Sciences, Kazan, 420083, Tatarstan, the Russian Federation.

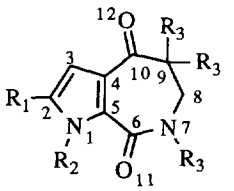

6 R_1=R_2=R_3=H
7 R_1=Br R_2=R_3=H
8 R_1=Br R_2=R_3=Me
10 R_1=Br R_2=Me R_3=H

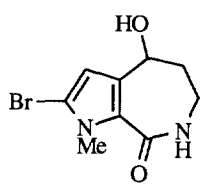

9

In the course of our work on marine natural products, we have isolated aldisin (**6**) and 2-bromoaldisin (**7**)[10 a, b] from a sponge of the class Demospongia and shown to have cytotoxic activity *in vitro*. The pyrrolo [2,3-c] azepine skeleton of **6** and **7** is structurally very similar to the imidazo [4,5-e][1,4] diazepine skeleton of **3**, **4** and **5**, thus suggesting aldisins **6** and **7** could be potentially useful simpler models of ring-expanded nucleosides.

In order to determine the extent of the structural analogy, we decided to compare the conformational composition of aldisin (**6**), 2-bromoaldisin (**7**), its methylated derivatives **8** and **10** and the alcohol **9** with that of ADA inhibitors **1-5**. Herein we report the results of empirical (MM) and semi-empirical (AM1) calculations and experimental DNMR studies.

Preparation of 6-9

Aldisin (**6**) and 2-bromoaldisin (**7**) were isolated from the sponge *Pseudaxinyssa sp.* and carefully purified. Optical rotation, $[\alpha]_{25}$=-6° and $[\alpha]_{25}$=+5° respectively, had been reported for these alkaloids[10b] probably due to the presence of impurities. HPLC purified samples from *Pseudaxinyssa cantharella* were found to be identical in all aspects to **6** and **7** isolated from *Pseudaxinyssa sp* (this work) and optically inactive. We give in the experimental part a full description of the isolation and purification procedures. Compound **8** was prepared by selective methylation of **7** with MeI/NaH and compound **10** by methylation with MeI/K_2CO_3 or with diazomethane, contrary to former results with a similar compound[10b]. The alcohol **9** was obtained by reduction of **7** with $NaBH_4$.

MM and Semi-empirical AM1 Calculations

Full conformational energy scans of **1-9** were carried out by MM and AM1 methodologies. For compounds **6**, **7** and **8**, MM calculations predicted two low energy conformations, which correspond to a pair of enantiomeric conformers. In both low energy conformations of **6** and **7**, the pyrrole and azepine rings are almost coplanar, but in the latter ring the lactam group and C(8) lie slightly out of the plane (torsion angles C(6)-C(5)-C(4)-C(10) and C(5)-C(6)-N(7)-C(8) are ca. 0.1 and 17°, respectively), and the N(7)-C(8)-C(9)-C(10) fragment is twisted, forcing the seven-membered ring into a twist-boat (TB) conformation (Figure 1). Ring inversion in **6** and **7** (TB-TB) proceeds via a boat (B) transition state conformation, and the energy barrier (calculated by MM) is ca. 12.5 kcal/mol. The lower energy and the transition state conformations of the

tetramethylated compound **8**, are similar to those of **6** and **7**, but the calculated energy barrier now is ca. 2.7 kcal/mol higher.

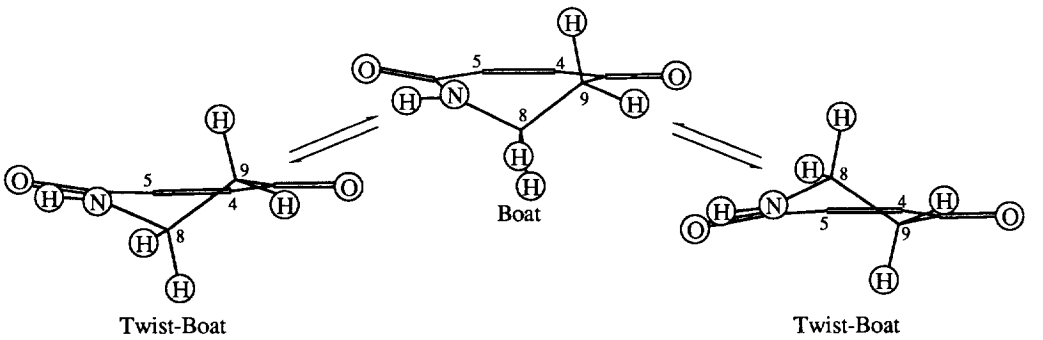

Fig. 1 Conformational equilibria of the seven-membered ring of aldisin (**6**) and 2-bromoaldisin (**7**).

In the case of the bromoalcohol **9**, MM calculations predict four low energy conformations: two twist-boat, TB_{eq} and TB_{ax}, and two boat conformers, B_{eq} and B_{ax}, in which the C(10)OH group is either pseudoequatorial (eq) or pseudoaxial (ax), (Figure 2). The TB_{eq} conformation is the lowest energy one, although it is only slightly more stable than the twist-boat conformation with the hydroxyl group pseudoaxial TBax. The energies of the boat conformations are higher than those of the twist-boats, and slightly lower than those of the distorted boat representing the transition state of TB-B interconversion. MM suggests that the TB_{eq}-TB_{ax} ring inversion may go via either B_{eq} or B_{ax} intermediates. In either case the exchange constants are higher than for dicarbonylic compounds **6-8**.

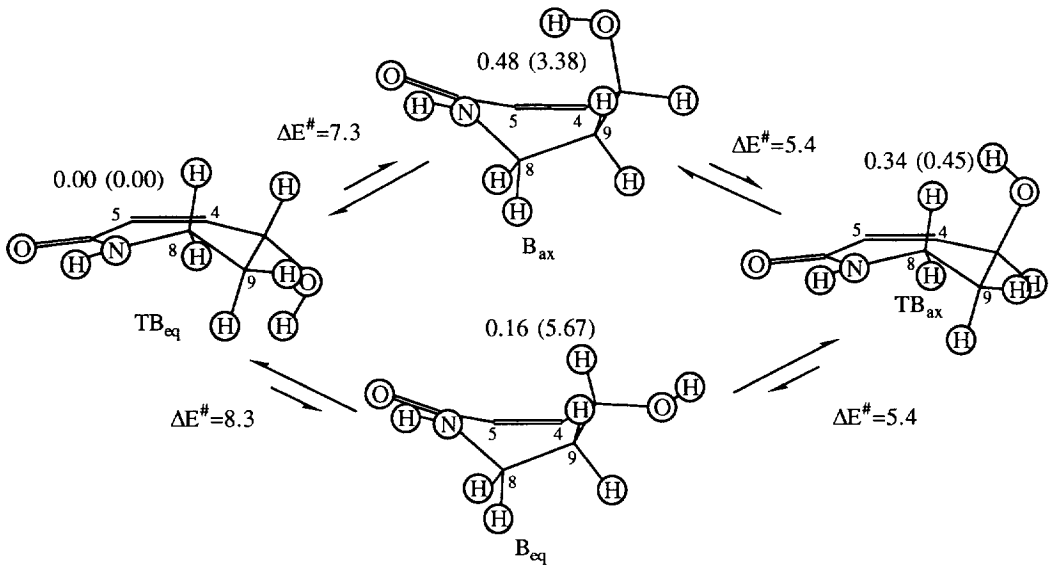

Fig. 2. Conformations and energy (kcal/mol) barriers of **9** as predicted by MM. The relative conformational energies of each conformer were calculated by AM1 and MM (in parenthesis).

The above MM derived results are corroborated by semi-empirical AM1 calculations, which predict three stationary points on the potential energy surface for the conformational equilibria of **6-8**. Two of these points correspond to geometries very close to the TB conformations predicted by MM (torsion angles C(6)-C(5)-C(4)-C(10) and C(5)-C(6)-N(7)-C(8) are ca. 0.1 and 1.1°, respectively); the third point corresponds to the boat-like transition-state[11] conformation between the two TB conformations (Figure 1). In the latter structure, the N(7)-C(8)-C(9) fragment lies above the plane of the pyrrole ring, and the O(6) and O(10) atoms below and therefore several torsion angles of the azepine are distorted.

AM1 predicts geometries for **9** which closely correspond to the B and TB conformations shown in Figure 2, although there is a slight difference in energy preference: both AM1 and MM give TB_{eq} as the major conformer, but respectively indicate that B_{eq} or TB_{ax} is the second most highly populated conformation (see Figure 2).

Finally, in **1**, **2**, **4** and **5** both MM and AM1 suggest a boat as the more stable conformer and an energy barrier for the inversion B_{ax}-B_{eq} of ca. 4.5 kcal/mol. In the case of azepinomycin (**3**) the most stable conformer is a twist-boat similar to that of **6** and the inversion barrier for TB_{ax}-TB_{eq} is calculated to be ca. 14.3 kcal/mol.

DNMR spectroscopy

The existence of conformational equilibria in the azepine rings of compounds **6** and **7** is evident from their room temperature ^{1}H-NMR spectra (Figure 3): the H(8) and H(9) protons of these compounds give signals characteristic of AA'BB' spin systems; if the azepine rings were totally rigid, they would exist in two enantiomeric conformations and their spectra would be more complex. In addition, the MM calculations suggest a fast conformational equilibria that should be slow at low temperature in compounds **6-8** only. To confirm that, we carried out ^{1}H-DNMR experiments on **6-9**.

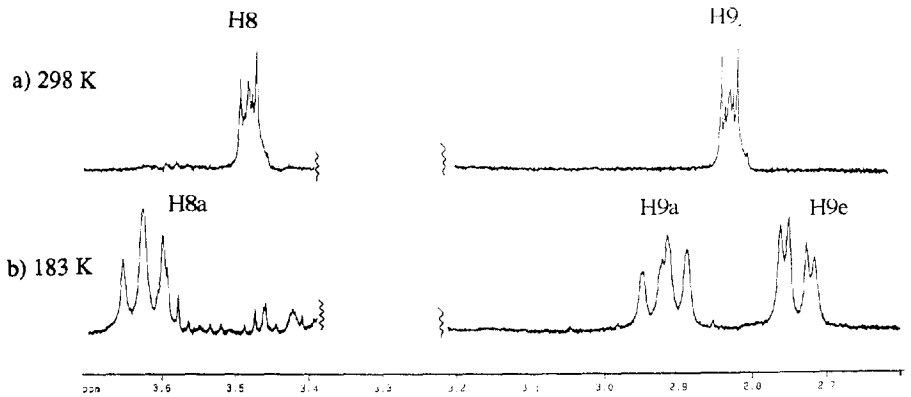

Fig. 3. Partial ^{1}H-NMR spectra of **6** in CD_3OD at: (a) 298 K; (b) 183 K.

In the room temperature ^{1}H-NMR spectrum of **6**, H(8) and H(9) appear as a AA'BB' spin system, the signals due to these protons being centred at 3.48 and 2.83 ppm, respectively. Between 223 and 183 K, evolution of signal lineshape is in keeping with a decreasing rate of a conformational equilibrium between two enantiomeric forms. At 183K, H(8) and H(9) give an ABCD spin system comprising signals due to H(8a) and H(8e) at 3.63 and 3.33 ppm, and H(9a) and H(9e) at 2.92 and 2.74 ppm, respectively. Lineshape analysis of the

spectrum obtained at 233 K allowed an estimation of the energy barrier for interconversion of the enantiomeric conformers (i.e. ABCD to BADC), which at that temperature had a value of ca. 10.6 kcal/mol (cf. 12.5 kcal/mol calculated by MM). For compound **7**, low temperature ^{1}H-NMR spectra and experimental energy barriers for conformer interconversion were similar to those of **6**.

The room temperature ^{1}H-NMR spectrum of the tetramethylated aldisin derivative, **8**, consists of a set of sharp singlets at 6.66, 3.93, 3.25 and 1.28 ppm, which are assigned to H(3), N(1)Me, N(2)Me and Me(9), respectively, and a broadened singlet at 3.66 ppm due to the two H(8) protons. Decreasing the probe temperature to 253 K caused the H(8) and Me(9) signals to collapse; at 183K both H(8) protons appeared as doublets (^{2}J=-15.3 Hz) centered at 4.167 and 3.262 ppm (i.e. an AB spin system), and Me(9) appeared as a pair of singlets at 1.253 and 1.205 ppm. Lineshape analysis of the spectrum taken at 249 K yielded an energy barrier to conformer interconversion of 11.4 kcal/mol; this is just 1 kcal/mol higher than the experimental value obtained for **6** and **7**. The small differences between calculated and experimental energy barriers are not especially significant and could well be originated by solvent effects and/or inaccuracy of the force field parameters.

Vicinal coupling constants were calculated by means of a modified Karplus equation[12a,b], for the optimized geometries of **6** and **7** shown in Figure 2 and found in good agreement with those obtained experimentally from low temperature ^{1}H-NMR spectra. In Figure 4 the AM1-calculated torsion angles and the J_{exp} values for the TB conformation of **6** are shown. This geometry is also in very good agreement with X-Ray data[13, 14] (Table 1).

The room temperature ^{1}H-NMR spectra of alcohol **9**, consists of a set of multiplets at 1.99, 2.20 (H(9)), 3.18, 3.36 (H(8)) and 4.9 (H(10)) ppm (i.e. an ABDEX spin system). There are no noteworthy changes in the pattern of signals upon decreasing the probe temperature, and even at 183K, line broadening was insignificant, indicating that the barrier to ring inversion is much lower than in the ketones **6, 7** and **8.** Exchange average J(10,9) agrees well with the AM1-derived exchange value.

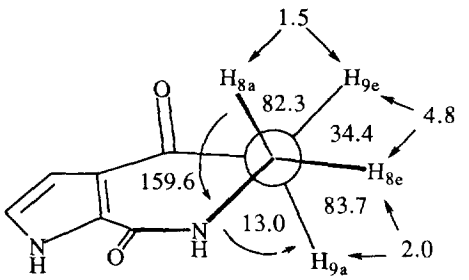

Fig. 4. AM1 calculated torsion angles and experimental coupling constants (Hz) for the N(7)-CH_2(8)-CH_2(9) fragment of the twisted-boat TB conformation of aldisin (**6**).

In summary, the ^{1}H-NMR experiments and calculations both indicate that aldisin (**6**) and 2-bromoaldisin (**7**) exist in solution as pairs of twist-boat conformers in equilibrium, and that these are in fact enantiomers which can interconvert via ring inversion. The low energy barrier to ring inversion (10.4 kcal/mol), indicates that this equilibrium will be relatively fast at room temperature, and so **6** and **7** should behave as racemic mixtures. The ground state conformational geometry obtained for the tetramethylated compound, **8**, is essentially the same as that of **6** and **7**, although the energy barrier to ring inversion is slightly higher (11.4 kcal/mol); compound **9**, is involved in a much faster conformational equilibria between two TB and two B conformations.

For its part, the calculated conformational geometries of **1-5** also showed good agreement with ^{1}H-NMR data. Coupling constants calculated for the two boat-like conformations B_{ax} and B_{eq} of **1** and **2** (^{3}J(7a,8)

B_{eq}=10.76 and $^3J(7e,8)$ B_{eq}=2.44 Hz, and $^3J(7e,8)$ B_{ax}=5.26 and $^3J(7a,8)$ B_{ax}=0.99 Hz) are in accordance with the experimental values[15a,b] ($^3J(7e,8)$=4.3 and $^3J(7a,8)$<1 Hz), confirming that the dominant conformation of coformycin (**1**) and pentostatin (**2**) closely correspond to the B_{ax} conformer illustrated in Figure 5. The calculated (AM1) energies suggest a 2:1 preference for the B_{ax} over the B_{eq} conformation, but a much stronger preference is deduced from the ^{1}H-NMR data. Solid state X-ray diffraction data[16] is also in keeping with a B_{ax} conformation.

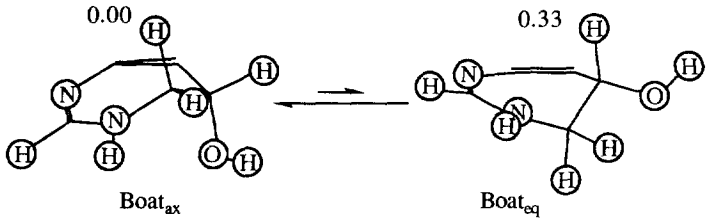

Figure 5. Low energy conformations and relative energies (kcal/mol; calculated by AM1) of the 1,3-diazepine ring of coformycin (**1**) and pentostatin (**2**).

For azepinomycin (**3**), AM1 calculated coupling constants ($^3J(5_a,6)$ TB_{eq}=2.22 and $^3J(5_b,6)$ TBeq=9.80 Hz, and $^3J(5_a,6)$ TBax=1.47 and $^3J(5_b,6)$ TBax=4.56 Hz) agree well with the experimental values[9a] ($^3J(5_a,6)$ is small and $^3J(5_b,6)$=5.4 Hz), for a twist-boat TB_{ax} with the C(6)OH group axial as dominant conformation (see Figure 6).

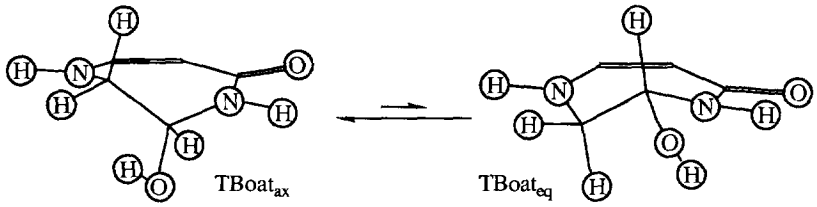

Figure 6. Low energy conformations of the 1,3-diazepine ring of azepinomycin (**3**).

These results indicate that the ring expanded nucleosides **1-2** adopt in solution a boat conformation Bax, and although compounds **6-8** present a twist-boat TB as the more stable conformer, the energy barrier to adopt a B conformation similar to that of **1-2** is low enough for it to be easily reached at room temperature (see Figures 1 and 5). The case of **9**, is similar but now the interconversion between B and TB conformers is easier. For its part, the conformation of azepinomycin **3** is not a boat, like **1** and **2**, but a twist-boat, TB, geometrically very similar to those of **6-9** (see Figures 1 and 6).

In conclusion, we found that aldisin and derivatives **6-9** present a high degree of conformational similarity with **1-5**, mainly with **3**, and that compounds with a pyrrolo [2,3-c] azepine system could be considered, at least from a conformational point of view, as good models for expanded nucleosides.

Experimental

Computational methods

Molecular Mechanics (CV force field[17]) and AM1 molecular orbital calculations were carried out using the Insight II package running on a Silicon Graphics Iris computer. Initial molecular geometries originated from the

Table 1. Selected torsion angles and coupling constants (Hz) for compounds **6, 7** and **9**.

	Calculated angles for **6** and **7**[a]		Calculated coupling constants for **6** and **7**[a]		Observed coupling constants for **6** and **7**[a]	
	MM	AM1	MM	AM1	T=193 K	T=303 K
8a8e	-	-	-	-	15.3	15.3 (15.3)
8a9a	168.9 (168.8)	159.6 (159.6)	12.21 (9.21)	10.95 (9.13)	13.0	9.27 (9.28)
8a9e	75.5 (75.6)	82.5 (82.4)	0.83 (1.02)	0.42 (0.50)	1.5	1.58 (1.60)
8e9a	76.5 (76.6)	83.7 (83.7)	1.21 (1.02)	0.58 (0.50)	2.0	1.58 (1.60)
8e9e	39.1 (39.0)	34.1 (34.3)	6.21 (9.21)	7.31 (9.13)	8.5	9.27 (9.28)
9a9e	-	-	-	-	17.0	17.0 (17.0)

	Calculated angles for conformers of **9**						Calculated coupling constants for conformers of **9**						Coupling constants for **9**		
													Calculated[b]		Observed
	TB eq		TB ax		B eq	B ax	TB eq		TB ax		B eq	B ax	303 K		303 K
	MM	AM1	MM	AM1	MM	AM1	MM	AM1	MM	AM1	AM1	AM1	MM	AM1	
8a8e	-	-	-	-	-	-	-	-	-	-	-	-	-	-	12.8
8a9a	165.4	157.8	167.8	157.8	65.7	63.6	11.72	10.61	11.99	10.67	1.73	2.02	10.19	7.84	9.51
8a9e	80.1	84.0	77.9	84.4	50.9	53.0	0.50	0.38	0.61	0.39	4.97	4.58	0.64	2.23	2.33
8e9a	80.0	85.5	78.1	85.2	50.5	52.8	0.79	0.50	0.94	0.52	4.22	3.80	0.74	3.78	2.74
8e9e	334.5	32.6	36.1	32.6	167.2	169.4	7.24	7.66	6.94	7.60	12.33	12.47	8.76	8.60	6.66
9a9e	-	-	-	-	-	-	-	-	-	-	-	-	-	-	14.3
9a10	169.5	174.3	52.4	39.5	145.4	22.8	10.84	11.18	2.85	4.55	7.41	7.17	8.55	6.61	6.10
9e10	55.1	57.3	61.4	77.0	28.7	92.6	4.85	4.60	3.68	1.97	8.57	1.16	4.21	6.10	6.20

[a] Data for **7** in parentheses.

[b] Exchange averaged values (MM and AM1 energy data, respectively).

Builder module of Insight II; 3D coordinates were then generated from the bond lengths and bond and dihedral angles by the DG-II package.[18] Analysis of the paths of conformer interconversion, and localization of ground state conformations were carried out by MM with an additional harmonic term of the form $k(1 + \cos(n\theta - \theta_0)$ included in the force field. Conformer energies were minimized in cartesian coordinate space by the block-diagonal Newton-Raphson method; minima corresponded to rms energy gradients < 0.001 kcal/mol. AM1 calculations were performed by the MOPAC 6.0 program: for all compounds, full geometry optimization was successfully achieved using the Broyden-Fletcher-Goldfarb-Shanno (BFGS) method and the PRECISE option.[19]

For transition state conformations, approximate Hessian (force-constant) matrices were used for geometry optimization, and stationary points on the potential energy surface were refined by minimization of the gradient norm using a non-linear least-squares method. The transition states were characterized by calculating the full Hessian matrix, diagonalizing it and establishing that there was only one negative eigenvalue[20].

NMR methods and calculations

^1H and ^{13}C NMR spectra of ca. 0.5 M sample solutions were recorded in a Bruker WM-250 spectrometer fitted with a 5 mm dual probe-head and operating at 250.132 MHz (^1H) and 62.9 MHz (^{13}C); pulse widths were calibrated to 30° flip angles; digital resolution was 0.2 Hz. For low temperature experiments, probe temperature was controlled by a standard unit calibrated using a methanol reference; samples were allowed to equilibrate for 15 min at each temperature before NMR data acquisition. Chemical shifts were referenced to TMS via solvent peaks.

^1H-NMR spectra at high (exchange averaged) and low (slow exchange) temperatures were processed on an Aspect 3000 computer and fitted with the Bruker simulation program PANIC. Good agreement between simulated and experimental spectra was obtained. Lineshape analysis of signals in exchange broadened spectra was carried out at intermediate temperatures (indicated in the text) by the DNMR5 program[21a,b]; rate constants for conformer equilibria were obtained from this data and used to calculate activation parameters by means of the Eyring equation[22].

General

Optical rotation were recorded in a Perkin-Elmer 141 polarimeter; UV spectra were recorded in a Perkin-Elmer Model 8452 A spectrophotometer; LREIMS were run in a Hewlett-Packard HP59970 spectrometer at 70 eV energy and HREIMS were run in a Kratos MS50 mass spectrometer; HPLC separations were performed on a Waters Model 6000A apparatus equipped with an R401 differential refractometer using μ-Bondapack C18 (7.8 mm i.d. x 30 cm) and Partisil M9 10/50 ODS-3 (9.4 mm i.d. x 50 cm) reverse phase columns.

Extraction and isolation

The sponge (*Pseudaxinyssa sp*, class Demospongia, order Axinellida) was collected off the island of Borneo by scuba divers. The sponges (2.2 Kg fresh weight) were freeze-dried and extracted with three 2 L portions of methanol, which were then concentrated to a viscous residue (6.75 g); these crude extracts exhibited cytotoxicity *in vitro* (82% and 70% inhibition of P388 and KB cells) and antimicrobial activity.

The extracts were dissolved in 200 mL of 9:1 MeOH/H_2O and this solution was subjected to the following series of solvent partitions: extract with two 200 mL portions of hexanes; add 25 mL of H_2O and extract with two 200 mL portions of CCl_4; add a further 75 mL of H_2O and extract with two 200 mL portions of CH_2Cl_2; after selectively evaporating the methanol at reduced pressure, the aqueous layer was extracted with four 200 mL portions of n-BuOH. Each of the organic layers was concentrated affording 3.99 g of hexane-soluble extracts, 0.91 g of CCl_4 soluble extracts, 0.96 g of CH_2Cl_2 soluble extracts, and 0.80 g of n-BuOH-soluble extracts.

The n-BuOH-soluble extracts were chromatographed on Amberlite XAD-2 (8 x 80 cm), eluting first with water (3.5 L), and then with MeOH (2 L). The methanol eluates were evaporated under reduced pressure to afford a residue (0.3 g), which was chromatographed on Sephadex LH-20 (2 x 50 cm), eluting with 2:1 MeOH/H_2O (flow rate, 50 mL/h) and collecting 10 fractions. Fraction 6 was flash-chromatographed on silica gel (Merck 60, 70-230 mesh; 1x20 cm), eluting with 7:3:1 $CHCl_3$/MeOH/H_2O and the residue obtained from the first three fractions subjected to reverse phase HPLC on a Partisil M9 10/50 ODS-3 column. Elution with 65:35 MeOH/H_2O (flow rate, 2.5 mL/min) afforded pure compounds **6** (10 mg, t_R=11 min) and **7** (20 mg, t_R=13 min).

Aldisin 6: $[\alpha]_{25}$=0° (c=0.0041); UV (MeOH), λ_{max}=218, 246, 298 nm; HREIMS, *m/z*=163.9682, calcd *m/z*=163.9666 for $C_8H_8N_2O_2$; LREIMS, *m/z* (relative intensity, %)=164 (100), 136 (39), 107 (52), 93 (64), 79 (33), 65 (19); ^{1}H-NMR (CD_3OD), δ_H=2.81 (m, 2H), 3.50 (m, 2H), 6.72 (d, 1H, J=3 Hz), 7.01 (d, 1H, J=3 Hz).

2-bromoaldisin 7: $[\alpha]_{25}$=0° (c=0.0031); UV (MeOH), λ_{max}=214, 236, 306 nm and (MeOH/NaOH), λ_{max}=214, 286, 346 nm; HREIMS, *m/z*=241.9650, calcd *m/z*=241.9690 for $C_8H_7{}^{79}BrN_2O_2$; LREIMS, *m/z* (%)=244-242 (100), 216-214 (48), 187-185 (51), 173-171 (49), 159-157 (36), 145-143 (12); ^{1}H-NMR (CD_3OD), δ_H=2.83 (m, 2H), 3.43 (m, 2H), 6.66 (s, 1H); ^{13}C-NMR (CD_3OD), δ_C=38.1, 44.3, 108.9, 113.0, 126.7, 130.3, 163.8, 196.0.

Preparation of 8. A solution of **7** (3 mg) in 2 mL of anhydrous THF, NaH (0.5 mg) and MeI (0.5 mL) were stirred at 60°C under an argon atmosphere for 13 h. The reaction mixture was concentrated *in vacuo* and the residue was diluted with 2 mL of water and then extracted with three 3 mL portions of diethyl ether. The combined ethereal layers were dried with anhydrous Na_2SO_4, concentrated *in vacuo* and chromatographed by reverse phase HPLC on a Partisil M9 10/50 ODS-3 column eluting with 85:15 MeOH/H_2O (flow rate, 2 mL/min) affording **8**, t_R=19 min, LREIMS, *m/z* (%)=300-298 (58), 257-255 (100), 244-242 (70), 229-227 (16), 216-214 (28), 200-198 (42), 188-186 (43). ^{1}H-NMR (CD_3OD) δ_H=1.28 (s, 6H), 3.25 (s, 3H), 3.66 (s, 2H), 3.93 (s, 3H), 6.66 (s, 1H).

Preparation of 10. Under an argon atmosphere, a solution of **7** (9 mg) in 2 mL of anhydrous DMF, K_2CO_3 (0.5 mg) and MeI (1 mL) were stirred at room temperature for 36 h. The reaction mixture was extracted with two 2 mL portions of CH_2Cl_2, which were dried with anhydrous Na_2SO_4 and concentrated *in vacuo*. The residue was chromatographed by reverse phase HPLC on a μ-Bondapack C18 column, eluting with 80:20 MeOH/H_2O (flow rate, 5 mL/min) producing compound **10** (8 mg), t_R=5 min, UV (MeOH), λ_{max}=228, 302 nm; HREIMS, *m/z*=255.9896, calcd. *m/z*=255.9846 for $C_9H_9{}^{79}BrN_2O_2$; LREIMS, *m/z* (%)=258-256 (100), 230-228 (46), 201-199 (64), 173-171 (40), 144-142 (11); ^{1}H-NMR (CD_3OD), δ_H=2.77 (m, 2H), 3.49 (m, 2H), 3.93 (s, 3H), 6.72 (s, 1H); ^{13}C-NMR (CD_3OD), δ_C=35.9, 38.1, 45.9, 112.5, 113.3, 127.6, 129.6, 164.5, 196.8.

Compound **10** was obtained also (90% yield) by treatment of **7** (7 mg in 1 mL of THF) with a solution of CH_2N_2 in ether (20 h at r.t.).

Preparation of 9. $NaBH_4$ (2 mg) was added to a solution of **10** (2 mg) in 0.5 mL of methanol and stirred at room temperature for 2h. Water was added to destroy excess borohydride, and the solution was concentrated and then extracted with three 2 mL portions of EtOAc. The combined organic layers were dried with anhydrous Na_2SO_4, concentrated *in vacuo* and chromatographed by reverse phase HPLC on a Partisil M9 10/50 ODS-3 column (9.4 mm x 50 cm) eluting with 80:20 MeOH/H_2O (flow rate, 2 mL/min), yielding compound **9** (2 mg), t_R=18 min. LREIMS, *m/z* (%)=260-258 (100), 241-239 (20), 230-228 (32), 214-212 (45), 203-201 (50),

161-159 (35), 188-186 (86); ^{1}H-NMR (CD_3OD) δ_H=1.99 (m, 1H), 2.20 (m, 1H), 3.18 (m, 1H), 3.36 (m, 1H), 3.83 (s, 3H), 4.90 (m, 1H), 6.36 (s, 1H).

Acknowledgements

This work was financially supported by the CICYT (SAF 92-1023) and Xunta de Galicia (XUGA 20907B/93). S.L.acknowledges the Spanish Ministry for Education and Science for a postdoctoral research grant. R. F. acknowledges a fellowship from the Xunta de Galicia. We thank Dr. Alain Ahond and Dr. Christiane Poupat for authentic samples of **6** and **7**.

References and notes

1. Walpole, C. S. J;.Wrigglesworth, R. *Nat. Prod. Rep.* **1989**, 6, 312-346.
2. Wolfenden, R.; Kati, W. M. *Acc. Chem. Res.* **1991**, 24, 209-215.
3. Wilson, D. K.; Rudolph, F. B.; Quiocho, F. A. *Science* **1991**, 252, 1278.
4. Hosmane, R. S.; Bhan, A.; Karpel, R. L.; Siriwardane, U.; Hosmane, N. S. *J. Org. Chem.* **1990**, 55, 5882-5890.
5. Jones, A. S. *Int. J. Biol. Macromol.* **1979**, 1, 194-207.
6. Acevedo, O. L.; Krawczyk, S. H.; Townsend, L. B. *J. Org. Chem.* **1986**, 51, 1050-1058.
7. Bridson, P. K., Lamberd, S. J., *J. Chem. Soc., Perkin Trans 1* **1990**, 173-175.
8. Hosmane, R. S.; Bhadti, V. S. and Lim. B. B. *Synthesis* **1990**, 1095-1100.
9. a) Isshiki, K.; Takahashi. Yo.; Iinuma. H.; Naganawa, H.; Umezawa, Yo.; Takeuchi, T.; Umezawa, H.; Nishimura, S.; Okada, N.; Tatsuta, K. *The J. of Antibiotics*. **1987**, 40, 1461-1463.
   b) Fujii, T.; Saito, T.; Fujisawa, T. *Heterocycles* **1988**, 27, 1163-1166.
10. a)Schmitz, F. J.; Gunasekera, S. P.; Lakshmi, V.; Tillekeratne, L. M. V. *J. Nat. Prod.* **1985**, 48, 47-53.
    b)de Nanteuil, G.; Ahond, A.; Guilhem, J.; Poupat, C.; Tran Huu Dau, E.; Potier, P.; Pusset, M.; Pusset, J.; Laboute, P. *Tetrahedron* **1985**, 41, 6019-6033.
11. For the boat-like geometry, the force-constant matrix had one negative eigenvalue, which is indicative of a transition state; the other two points have no negative eigenvalues, and correspond to energy minima (see ref. 20).
12. a) Haasnoot, C. A. G.; DeLeeuw, F. A. A, M.; Altona, C. *Tetrahedron* **1981**, *36*, 2783-2792.
    b) Garbish, E. W. *J. Am. Chem. Soc.* **1964**, 86, 5561-5564.
13. Mattia, C.A.; Mazzarella, L.; Puliti, R. *Acta Cryst.* **1982**, B38, 2513-2515.
14. Kitagawa, I.; Kobayashi, M.; Kitanaka, K.; Kido, M.; Kyogoku, Yo. *Chem. Pharm. Bull.* **1983**, 31, 2321-2328.
15. a) Chan, E.; Putt, S.R.; Showalter, H.D. H.; *J. Org. Chem.* **1982**, 47, 3457-3464.
    b) Woo, P. W. K.; Dion, H. W.; Lange, S. M.; Dahl, L. F.; Durham, L. J. *J. Heterocyclic Chemistry* **1974**, 11, p.641-643.
16. Nakamura, H.; Koyama, G.; Iitaka, Yo.; Ohno, M.; Yagisawa, N.; Kondo, Sh.; Maeda, K.; Umezawa, H. *J. Am. Chem. Soc.* **1974**, 96, 4327-4328.
17. Roberts, V.A.; Osguthorpe, D.I.; Wolff, J.; Genest, M.; Hagler, A.T. *Proteins: Structure, Function and Genetics* **1988**, 4, 31.
18. Havel, T. F.; *Prog. Mol. Biol. Biophyl.* **1991**, 56, 43-78.
19. Cioslowski, J.; Kertesz, M. *QCPE Bull.* **1987**, 7, 159.
20. Komorinski, A.; Mclver, J. W. Jr. *J. Am. Chem. Soc.* **1973**, 95, 4512-4517.
21. a) Binsch, G.; *J. Am. Chem. Soc.* **1969**, 91, 1304-1309.
    b) Kleier, D. A.; Binsch, G.; *J. Magn. Res.* **1970**, 3, 146-160.
22. Friebolin, H. P. Basic one- and two-dimentional NMR Spectroscopy. Weinheim: VCH, 1991.

(*Received in UK* 13 *September* 1994; *revised* 16 *November* 1994; *accepted* 18 *November* 1994)